

VELOCITY MEASUREMENT AROUND A LARGE BUBBLE RISING IN STAGNANT WATER IN A ROUND PIPE USING THE UVP

Hisato Minagawa*, Masaya Ibuki**, Satoshi Yamada***, Yoichi Shiomi****

* Department of Mechanical Systems Engineering, The University of Shiga Prefecture,
2500 Hassaka, Hikone, Shiga 522-8533, JAPAN, E-mail: minagawa@mech.usp.ac.jp

** Dainippon Screen MFG Co. Ltd., Tenjinkita-cho 1-1, Teranouchi-agaru
4-chome, Horikawa-dori, Kamigyo-ku, Kyoto 602-8585, JAPAN

***Engineering Graduate School, The University of Shiga Prefecture,
2500 Hassaka, Hikone, Shiga 522-8533, JAPAN, E-mail: satoshi@cont4.mech.usp.ac.jp

**** Department of Mechanical Systems Engineering, Ryukoku University,
1-5 Yokotani, Seta Oe-cho, Otsu, Shiga 520-2194, JAPAN, E-mail: shiomi@rins.ryukoku.ac.jp

ABSTRACT

A UVP measurement was performed to obtain the liquid velocity field in front of, around and behind the large bubble rising in stagnant water in a round pipe of $D=54\text{mm}$ in order to get basic information for the gas-liquid two-phase slug flows. It is also useful if we can establish the measuring technique of the subject by a more convenient but precise measuring technique. Two ultrasonic transducers were used simultaneously for the measurement to get velocity vectors. The measured results are presented and compared with some existing studies on the corresponding phenomena. In the liquid film near the bubble nose, velocity profile and acceleration are presented and compared with existing studies. The different in D may affect some features. The parameter z/D is found more dominant than z for this phenomenon. In the liquid phase behind the bubble tail or the wake region, a large ring vortex is recognized without another weaker vortex behind it. The upward velocity near the pipe axis agrees well with the predicted results by an existing prediction.

Keywords: Large Bubble, Multiphase flow, Velocity Vector, Vortex, Wake, Velocity Profile, UVP

INTRODUCTION

Gas-liquid two-phase slug flows in vertical pipes are frequently encountered in industrial pipelines, chemical and nuclear reactors and other fluid machineries. The flow is characterized by a series of bullet-shaped large bubbles or Taylor bubbles, and liquid slugs which contains small bubbles. In order to clarify the characteristics of the flow, a lot of studies have been performed [1]. The characteristics of the void fraction, the frictional pressure drop of the flow and the rising velocity of the large bubbles have been revealed considerably. The precise velocity field around the large bubbles in the slug flow, however, is not clarified so well. It is useful to know the velocity field around a large bubble rising in a stagnant liquid, which is one of the simplified forms of large bubbles in slug flows in vertical pipes. Even for the subject, few studies have been reported: for example, the measurement using photochromic dye activation method by Kawaji et al. [2] and that using PIV by van Hout et al. [3]. Tomiyama et al. [4] performed the measurements using LDV especially to clarify the flow field in the wakes behind the large bubbles.

Kawaji et al. [2] measured the velocity field around a large bubble rising through stagnant kerosene in a 25.6mm I.D. pipe. 0.01% TNSB, a photosensitive substance (photochromic dye) was dissolved beforehand and a periodic laser beam was used to expose the dye. van Hout et al.[3] measured the velocity field around a large bubble rising through stagnant water in a 25mm I.D. pipe. Polystyrol particles of 20 to 40 μm diameter containing fluorescent dye were added to the water, and PIV measurements were performed with the help of Laser-Induced-

Fluorescence. Their both studies presented velocity fields around a large bubble rising through stagnant liquid and also those in the liquid lump behind the bubble or the wake region. But the effects of the pipe diameter, the large bubble length, the liquid properties, the wall wettability, the existence of small bubbles in the liquid slug and so on, on the velocity field are not quite clear. So we still need a systematic and precise data base on the flow field. Moreover, we will need the velocity field in the two-phase slug flow in future in order to investigate the flow characteristics of the flow and to model the flow more precisely.

Hence we need a more convenient but precise measuring technique to achieve this purpose. The Ultrasonic Velocity Profile monitor (UVP) is one of the candidates, because it is easy to operate once the measuring technique is fixed, it has effective time and space resolutions, and it obtains velocity vectors on a line in an instant. In this paper, the UVP measurement was performed to measure the velocity field around a large bubble rising in stagnant water filled in a round vertical pipe so as to obtain basic information to establish the measuring technique of the subject.

EXPERIMENTAL METHOD

A schematic of the experimental apparatus is shown in Fig.1. Water filled in the tank was supplied by a Mohnno pump to the test section. Polyethylene particles of median diameter 160 μm were used for the scattering particles. The temperature of the water was kept at $20\pm 1^\circ\text{C}$ by a regulator. When the test section

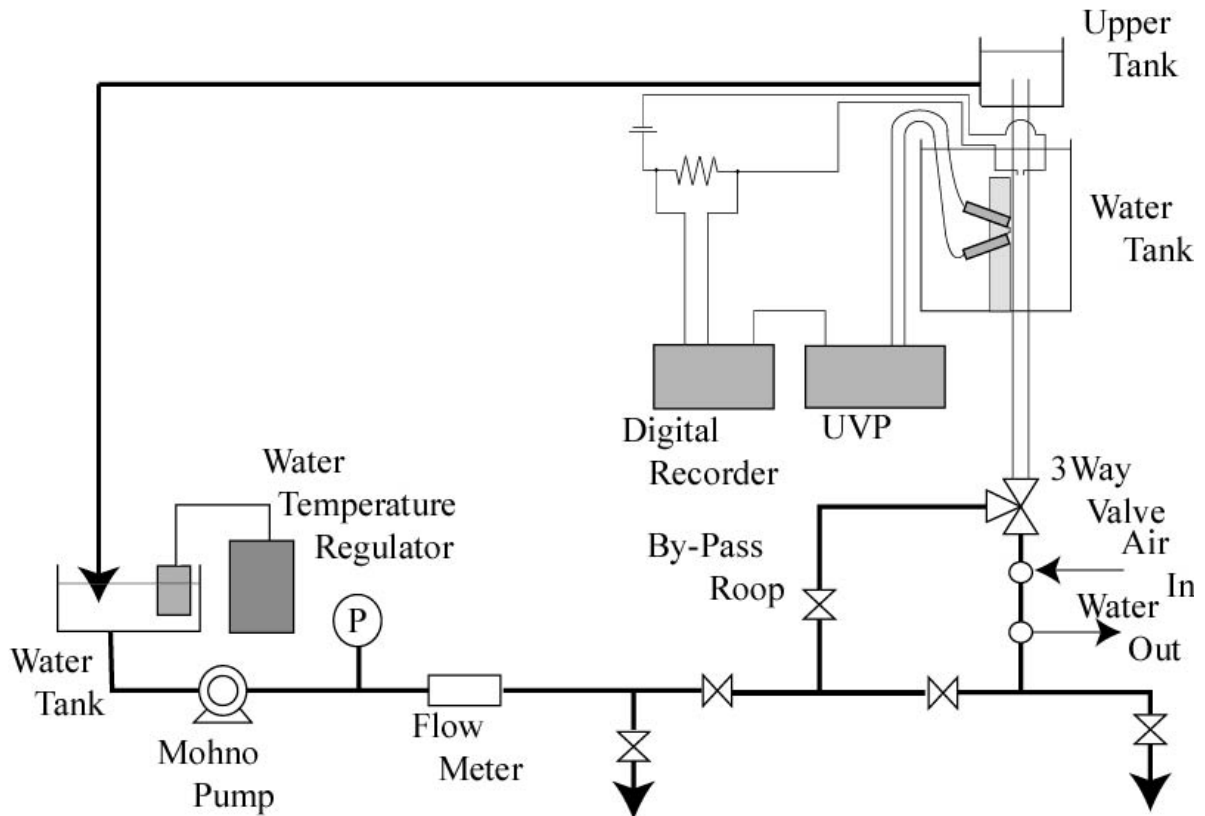


Fig.1 Experimental Apparatus

was fully filled by the water, the pump was stopped. The valves were once closed, and air was stored in the pipe just under the 3 way valve by draining water from the pipe.

The test section was consisted of a transparent acrylic vertical round pipe of 54mm I.D. and about 3m in length. Two ultrasonic transducers of UVP (frequency: 4MHz) were set at the outside of the test section at 2.3m from the 3 way valve: one +20 degree and the other -20 degree inclined from the horizontal line as shown in Fig.2. They were set in water in a tank, whose water surface was covered with a styrene foam sheet to prevent the noise caused by the shaking water surface. The measuring frequency of UVP was 50Hz. A pair of electrode was installed in the pipe 75mm downstream of the transducers to detect the relation between time and position of the large bubble, which is denoted by the large bubble sensor. Signals from UVP and the large bubble sensor were recorded simultaneously by a digital recorder.

When all the facilities were ready, 3 way valve was quickly opened, and a large bubble rose up into the test section, and signals were recorded. Velocity field for about 30 large bubbles were measured for one air volume in this study. The averaged large bubble length was 0.225m and the averaged terminal rising velocity of the large bubbles, V_{Bt} , was 0.269m/s, which is a reasonable value compared with some predicted values by existing methods for V_{Bt} [1].

After getting data for these 30 large bubbles, we obtained averaged velocity vectors. The velocity data were divided both for longitudinal and radial sections; divided into each 5.2mm for the longitudinal direction (Z axis), and into each 0.695mm for the radial direction (r axis) to make many cells. The Z - and r -components of the velocity were averaged for each cell.

The specification of the pipe wall position was performed using the measured data for the liquid single phase flow. Figure 3 exhibits a velocity profile of a liquid single phase flow by the same setup. Solid and open symbols are for the transducer of an elevation angle ($\theta=+20^\circ$) and for the transducer of a

depression angle ($\theta=-20^\circ$), respectively. The solid line is an approximation by the 1/7th power law. Although the data are scattered to a certain degree near the pipe wall at the far side of the transducer ($r/R=1$), we can easily find the wall position at the near side of the transducer ($r/R=-1$).

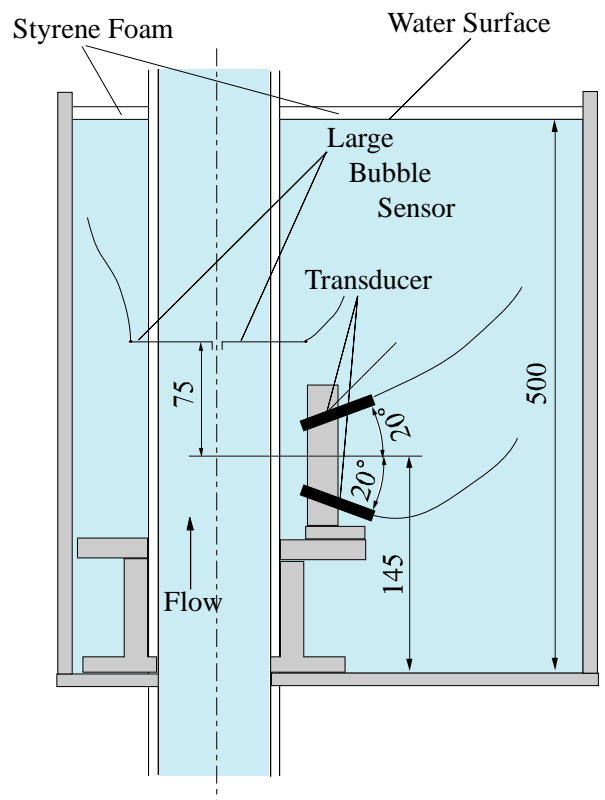


Fig.2 Test Section

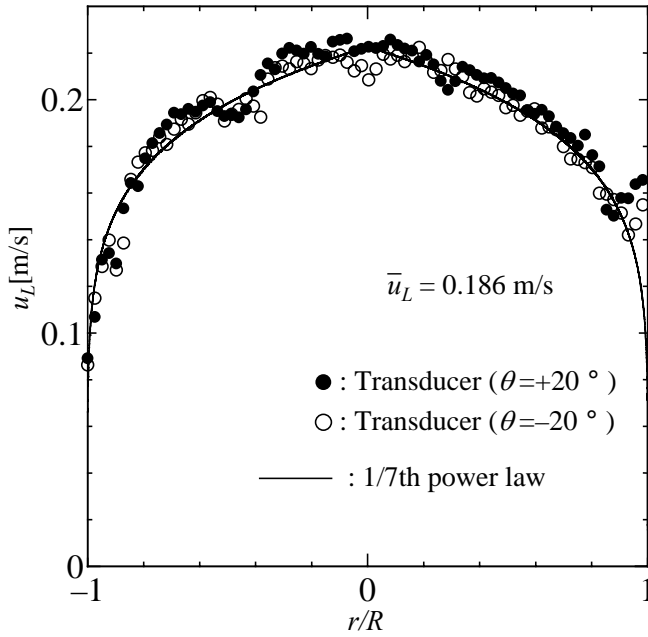


Fig.3 Velocity Profile of Liquid Single Phase Flow

RESULTS AND DISCUSSION

The obtained result of the velocity field is presented in Fig.4 (a) and (b). Figure 4 (a) shows the velocity field in the liquid phase in front of the large bubble, and that in the liquid film around the large bubble, whereas (b) shows the velocity field in the liquid phase behind the large bubble. Z denotes the downward distance from the tail of the large bubble and z from the nose. Only the measured data of the near side, i.e. the data from the wall at the near side of the transducer to the pipe center axis, are used in the figures below, and are copied to the other side under the assumption of the axial symmetry. The shape of the large bubble is estimated by the bubble shape function proposed by Nakahara et al. [5].

$$r/R = 0.9 - \left\{ (z/R)^{0.7} + 0.9^{-1/a} \right\} \quad (1)$$

$$a = \begin{cases} -3.26 \times 10^{-4} \text{Re} + 2.83 & (\text{Re} \leq 1550) \\ -2.29 \times 10^{-5} \text{Re} + 2.36 & (\text{Re} > 1550) \end{cases}$$

The gas-liquid interface is predicted to be at r in Eq.(1) with $\text{Re}=0$ because of stagnant water. All the velocity vectors in the large bubble were eliminated, although some vectors were obtained in it according to the error supposed to be occurred by the reflection of ultrasonic sound by the interface. Figure 4 is scaled with even intervals on both axes; the shape of large bubble is drawn in the correct aspect ratio.

Liquid Phase in front of Large Bubble

In the liquid phase in front of the large bubble, only very small velocity components are recognized. In order to make the flow field clear, we enlarged the velocity vector display in this region as shown in Fig.5. The effect of the rising large bubble is recognized to approximately $z = -0.025\text{m}$ from the bubble nose. It corresponds nearly $D/2$ from the nose, where $D=2R$ is the pipe diameter, which is the same result as van Hout et al. [2]. In this effected region, the liquid near the pipe axis is lifted owing to the rising bubble nose, whereas near the pipe wall, the downward flow is recognized, which will flow into the liquid

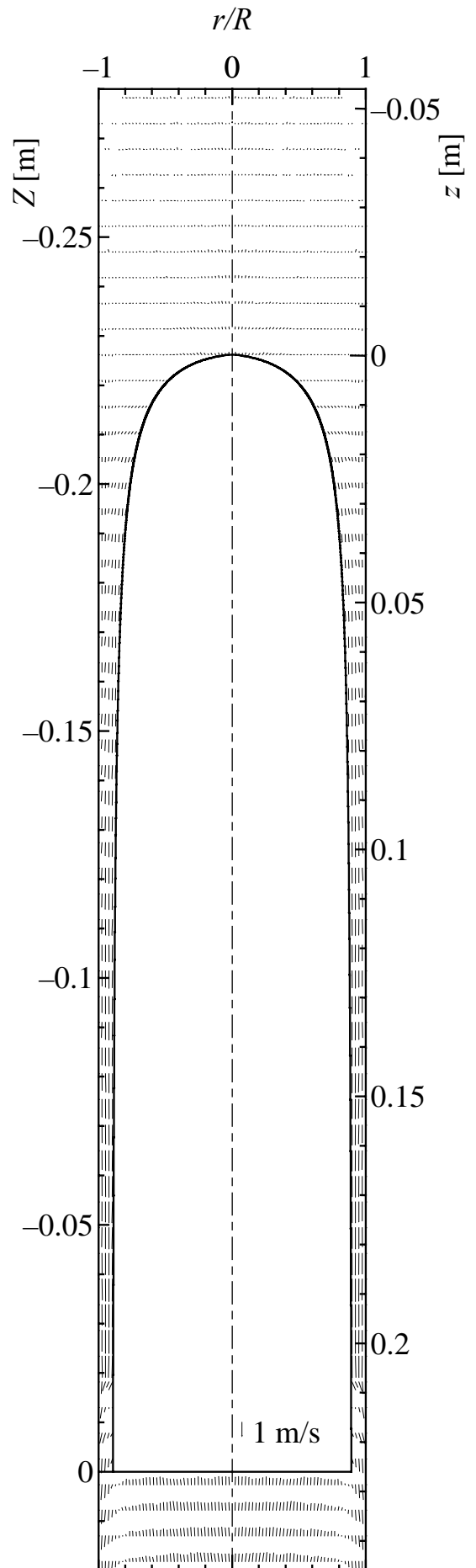


Fig.4 (a) Velocity Field (Around Large Bubble)

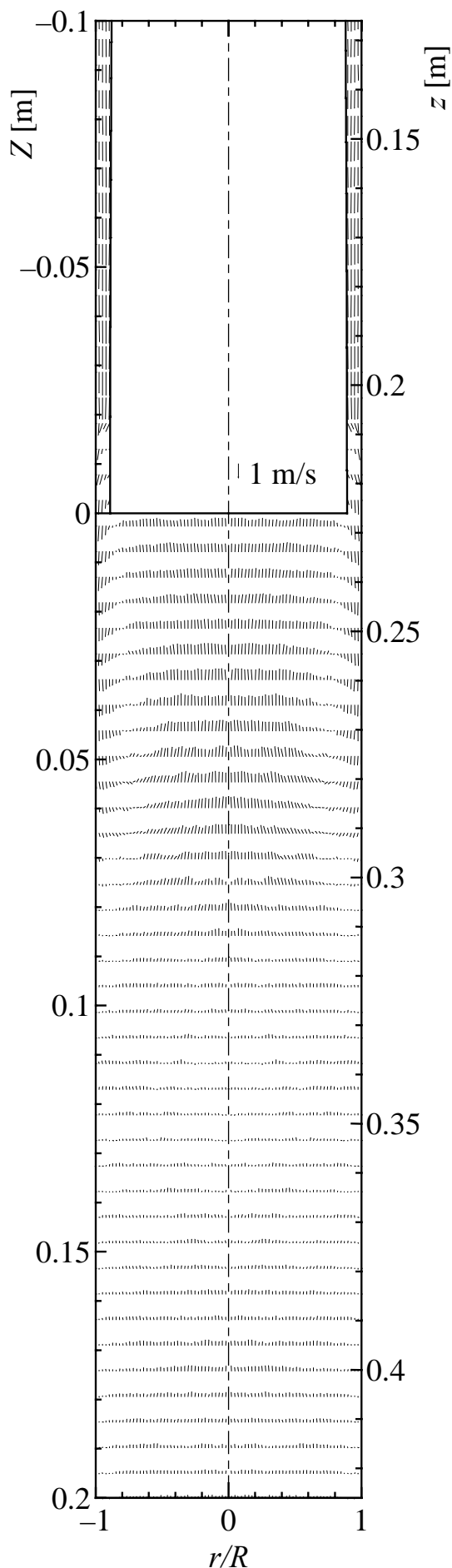


Fig.4 (b) Velocity Field (Behind Large Bubble)

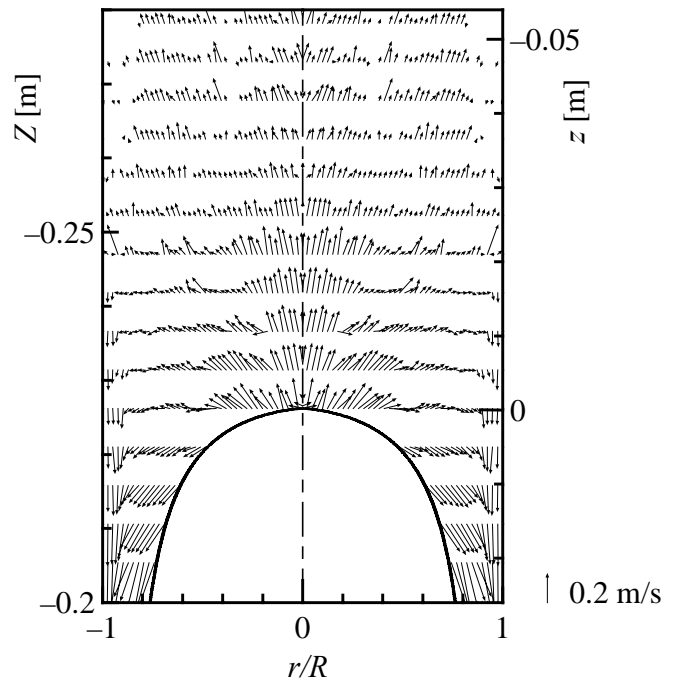


Fig.5 Velocity Field in Front of the Large Bubble

film around the large bubble, which also agrees with the findings of van Hout et al.

Liquid Film around Large Bubble

In the liquid film near the bubble nose, the velocity vectors near the pipe wall are almost vertically downward, but those near the gas-liquid interface are toward its tangential direction; they tend to shift the direction to the vertical downward direction as they travel downward. At the midway of the large bubble length, they are fully vertically downward as shown in Fig.6. The downward velocity slightly increases from the pipe wall ($r/R=-1$) to the gas-liquid interface. At the interface, the velocity gradient is, however, negligible so that the shear stress is also negligible. The velocity profiles in the liquid film are shown and are compared with van Hout's and Kawaji's results in Figs.7 & 8. The plotted data, u_L , are obtained as the axial downward component of the velocity vectors. We can recognize the velocity profiles in the liquid film have the maximum values at the interfaces. In Fig.7, the figure parameter is z . In this case, the velocities measured in this study are smaller than van Hout's and Kawaji's data for the same value of z . The difference is more remarkable when z is smaller. Thus, even if the distance from the nose is the same, the liquid velocity in the film falls faster when D is smaller.

Figure 8 is the similar plot with z/D as parameter instead of z in Fig.7. When the value of z/D is smaller than unity, the velocity profiles of this study agree with the two existing studies to a certain degree. When it exceeds unity, the liquid velocities in this study are longer than them. This is probably because of the difference in pipe diameters. Although van Hout's and Kawaji's measurements were based on around $D=25\text{mm}$ pipe, our UVP measurement was performed for $D=54\text{mm}$ pipe. Thus, the parameter z/D is more dominant than z itself especially when z/D is less than unity.

The maximum downward velocities, $u_{L, \max}$, in the liquid film are plotted against Z and z in Fig.9. The liquid downward velocity of course increases as they travel downward. As the result, the film thickness becomes thin gradually. But the accelerations are somewhat different.

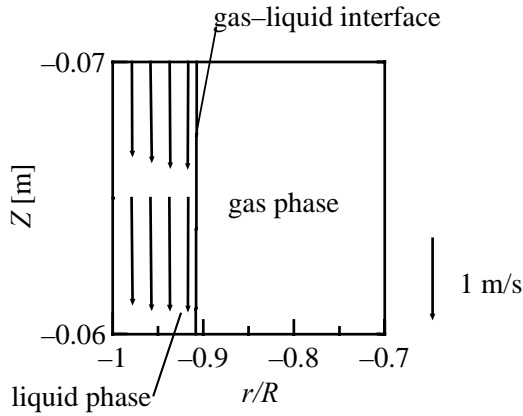


Fig. 6 Velocity Vectors in the Liquid Film around the Large Bubble

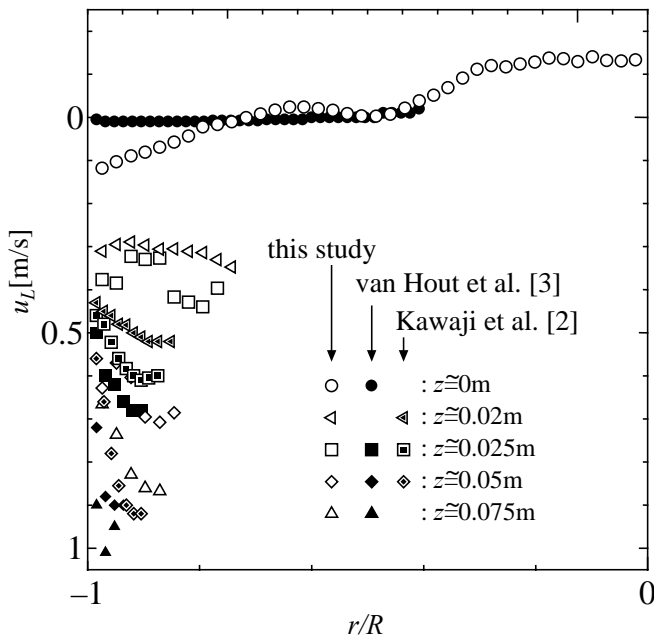


Fig. 7 Velocity Profiles in the Liquid Film with z as Parameter

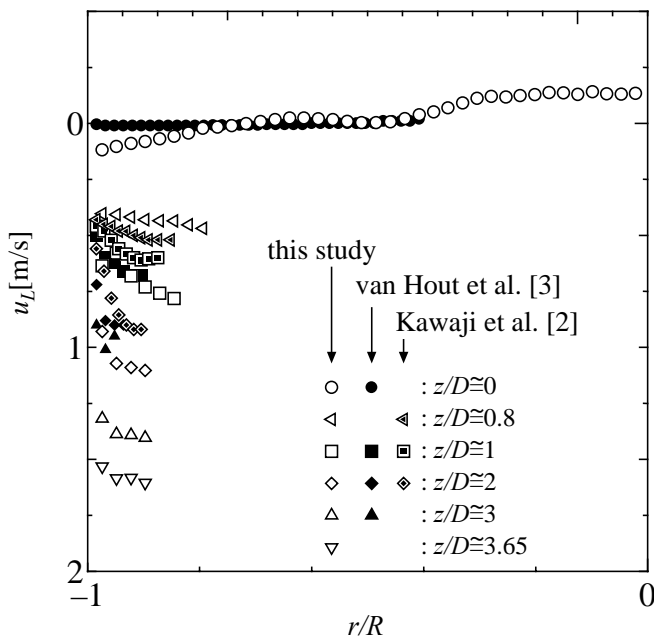


Fig. 8 Velocity Profiles in the Liquid Film with z/D as Parameter

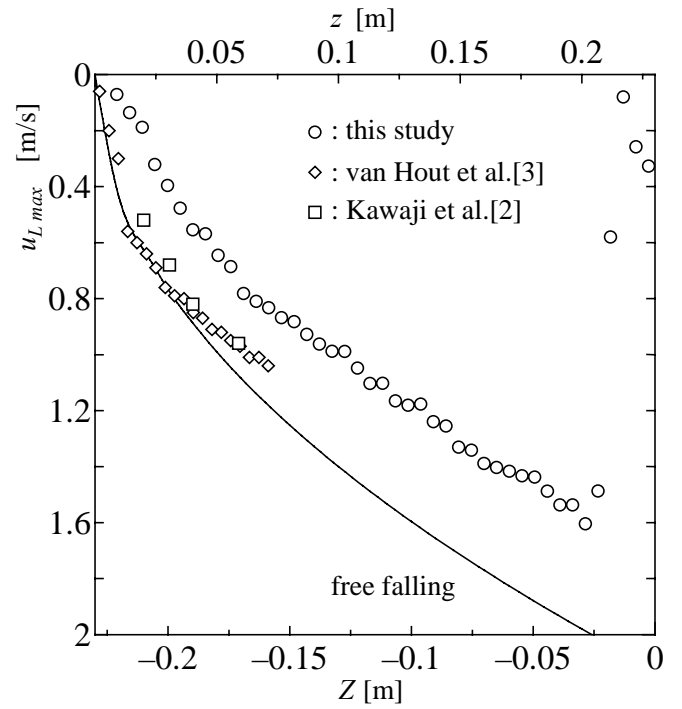


Fig. 9 Maximum Downward Velocities in the Liquid Film

For smaller pipe diameters ($D \approx 25\text{mm}$), the accelerations are approximately g near the bubble nose ($z < 2.5\text{cm}$). But their data soon begin to depart from the free falling curve. The acceleration is repressed probably according to the viscous force. In our data for larger pipe diameter ($D = 54\text{mm}$), the effect is more remarkable. The value of acceleration is smaller than g even near the bubble nose. In the region near the bubble tail ($z > 0.2$), the values of $u_{L,max}$ suddenly decreases. It does not mean the liquid film decelerates; acceleration continues to the bubble tail at least for each large bubble. But due to the vigorous oscillations of bubble tail, the averaged values of u_L in this region decreases drastically. The difficulty in measuring velocity here was also pointed out by van Hout et al. [3].

Liquid Phase behind Large Bubble

The liquid falling down in the film penetrates into liquid phase behind the large bubble to make a wake region as shown in Fig. 4 (b). On the other hand, upward velocity is observed near the pipe axis. These flows form a ring vortex whose longitudinal length is about 0.08m or $1.5D$. The corresponding value by van Hout et al. [3] was $2D$, which is not different so much, whereas we do not find another weaker vortex they identified below the first vortex.

The upward velocity near the pipe axis was studied and related to large bubble length by Tomiyama et al. [4]. Figure 10 illustrates the upward liquid velocity at the pipe axis, $-u_{L,axis}$, with Tomiyama's predicted curve. They agree well qualitatively. About less than 0.07m from the large bubble tail is the near-wake region, where liquid upward velocity exceeds V_{Bt} or terminal rising velocity of the large bubble. Behind the near-wake region, we recognize the far-wake region where the upward velocity is decaying to zero. Thus, the near-wake region length has a similar value to that of the vortex size, 0.08m . This actual dimension is also close to that of van Hout, 0.10m .

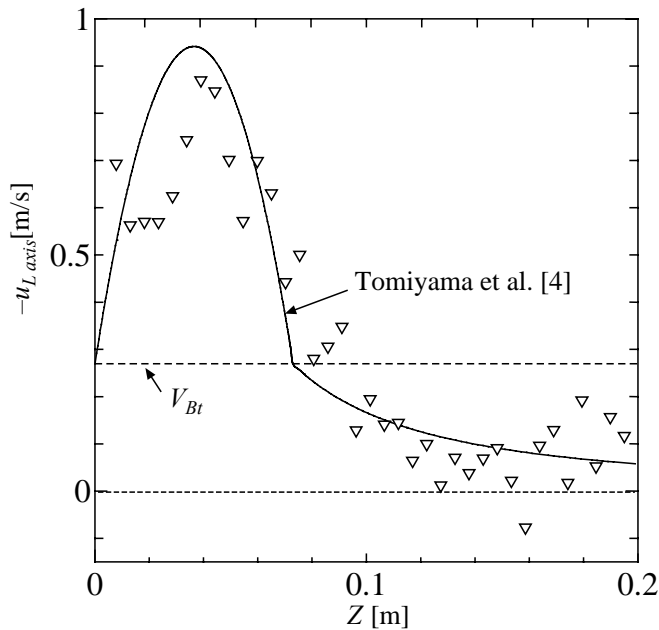


Fig.10 Upward Liquid Velocity at the Pipe Axis in the Wake

CONCLUDING REMARKS

A UVP measurement was performed for the liquid velocity field in front of, around and behind the large bubble rising in stagnant water in a round pipe of $D=54\text{mm}$. The measured results are presented and compared with some existing studies on the corresponding phenomena. In the liquid phase in front of the large bubble, the liquid near the pipe axis is lifted owing to the rising bubble nose, whereas near the pipe wall, the downward flow is recognized which will flow into the liquid film in the region $0.5D$ from the nose. In the liquid film near the bubble nose, velocity profile and acceleration are presented and compared with existing studies. The different in D may affect some features. The parameter z/D is found more dominant than z itself especially when z/D is less than unity. In the liquid phase behind the bubble tail or the wake region, a large ring vortex is recognized without another weaker vortex behind it. The upward velocity near the pipe axis agrees well with Tomiyama's prediction qualitatively. The near-wake region length has a similar value to that of the vortex size.

REFERENCES

1. JSME, 1995, Handbook of gas-liquid two-phase flow technology, Corona-sha, Tokyo (in Japanese).
2. M. Kawaji, J.M. Dejesus, G. Tudose, 1997, Investigation of flow structures in vertical slug flow, *Nuclear Engineering and Design*, 175, pp.37-48.
3. R. van Hout, A. Gulitski, D. Barnea, L. Shemer, 2002, Experimental investigation of the velocity field induced by a Taylor bubble rising in stagnant water, *International Journal of Multiphase Flow*, 28, pp.579-596.
4. A. Tomiyama, H. Tamai, S. Hosokawa, 2001, Velocity and pressure distribution around large bubbles rising through a vertical pipe, *proc. ICMF 2001*, New Orleans, in CD-ROM.
5. Y. Nakahara, G. Morita, A. Tomiyama, 2000, Study on shape and terminal rising velocity of single bubbles moving in a vertical pipe, *proc. annual meeting JSMF 2000*, pp.175-176 (in Japanese).

NOMENCLATURES

D	: pipe inner diameter	[mm]
g	: gravitational acceleration	$[\text{m/s}^2]$
r	: radial distance from the pipe axis	[mm]
R	: pipe radius ($=D/2$)	[mm]
u_L	: axial component of local liquid velocity	[m/s]
V_{Bt}	: terminal rising velocity of a large bubble	[m/s]
z	: longitudinal distance from the bubble nose	[m]
Z	: longitudinal distance from the bubble tail	[m]

ACKNOWLEDGEMENT

The authors would like to acknowledge Dr. H. Kikura of TIT for his helpful advice on the measuring technique by UVP. We also express our gratitude to Mr. T. Kubota (Kanebo Foods) and Mr. T. Fukazawa (USP) who performed some of experimental works for this study.